JOURNAL OF MATERIALS SCIENCE 15 (1980) 2720–2728

Formation of metastable solid solutions in the Pb–Ge system

DILSHAD AKHTAR, T. C. GOEL, V. D. VANKAR, K. L. CHOPRA
Indian Institute of Technology, Hauz Khas, New Delhi-110029, India

The formation and decomposition behaviours of metastable solid solutions in liquid-quenched and vapour-quenched Pb–Ge alloys were studied using X-ray diffraction, transmission electron microscopy (TEM), differential thermal analysis (DTA) and resistance measurement techniques. It is shown that the Pb-rich fcc phase can retain upto about 13 at% Ge on liquid-quenching and upto about 5 at% Ge on vapour-quenching. Decomposition of the Pb-rich fcc phase occurs in the temperature range 220 to 300° C and it is a temperature dependent nucleation and growth phenomenon. Upto about 7.5 at% Pb can be retained in Ge-rich compositions in an amorphous Ge matrix on vapour-quenching but there is no detectable solubility of Pb in crystalline Ge retained by liquid-quenching. On heating, the amorphous Ge–Pb films crystallize to a Ge-rich solid solution which decomposes to equilibrium constituents at higher temperatures. Stability of amorphous Ge–Pb films decreases on increasing metal concentration.

1. Introduction

Rapid quenching of vapour/liquid has become an established method for freezing-in a high temperature state. Non-equilibrium crystalline and amorphous phases as well as supersaturated crystalline solid solutions have been produced by both vapour and liquid quenching techniques [1, 2]. The two processes, however, differ intrinsically, since vapour-quenching is an atom by atom deposition process and the structure of the vapour phase is probably not retained in the condensed solid whereas liquid-quenching is an attempt to "freeze-in" the liquid structure. A systematic comparison of metastable effects produced by the two methods has not been made so far.

Recently we reported the formation of non-equilibrium structures in liquid-quenched and vapour-quenched Pb and Sb [3–5]. To compare the effects of the two quenching processes on solid solubility and quenched products in alloys, we have studied the structure of liquid-quenched and vapour-quenched Pb–Ge alloys. The phase diagram of the Pb–Ge system [6] shows no solid solubility of Pb and Ge in each other under equilibrium conditions, and to our knowledge the formation of metastable solid solution in the Pb–Ge system has not so far been reported. In this paper we report our results on the formation and decomposition of metastable solid solutions in the Pb–Ge system.

2. Experimental procedures

Pb–Ge alloys were prepared in the whole composition range by melting the high purity constituents in evacuated and sealed quartz ampoules and then rapidly quenching the melt in water to minimize segregation. Liquid-quenched foils were prepared by the gun apparatus of splat-quenching descibed elsewhere [3]. Prior to the quenching operation, the apparatus was evacuated to about 10^{-2} Torr and continuously flushed with argon so as to maintain an argon pressure of about 5 Torr inside the chamber. The initial melt temperatures were about 50° C above the liquidus of the given alloy. A rupture pressure of about 80 kg cm^{-2} was employed to create a shockwave and eject the molten material from the crucible on to a water cooled curved copper substrate. The liquid-quenched foils could be easily stripped off the copper substrate. Vapour-quenched films were pre-

0022–2461/80/112720–09$02.90/0

pared in a high vacuum (about 10^{-6} Torr) by thermal evaporation from a resistively heated tungsten basket onto freshly cleaved NaCl crystals and properly cleaned microscope glass slides held at room temperatures. Experimental details have already been described by Chopra *et al.* [7]. The incidence of the vapour beam was kept normal to the substrates. A shutter was used to allow deposition only when the source material was completely degassed. High evaporation rates > 20 Å sec^{-1} were employed to maintain the stoichiometry of the film composition. The reproducibility of the data for films prepared sequentially from the same melt (until the whole of it was exhausted) indicates that the composition of the alloy is maintained in the film. The film thickness was about 1000 to 1200 Å.

The central regions of liquid-quenched foils provided, in some cases, good continuous specimens for electrical resistance measurements. A four-probe potentiometric technique was used for this purpose. Other portions of the central region were cut out for X-ray studies. Few samples were annealed at appropriate temperatures by heating in vacuum (about 10^{-2} Torr). Diffractometer traces of as-quenched and annealed samples were obtained with a Philips diffractometer at a scan rate of 1° (2θ) per min. Nickel filtered CuK_α radiation at 30 kV and 20 mA was used in all cases. Vapour-quenched films were, however, not suitable for X-ray examination.

Liquid-quenched and vapour-quenched samples were examined in an AEI EM 802 transmission electron microscope operating at 80 kV. Thin edges of the liquid-quenched foils were suitable for direct transmission electron microscopy (TEM) studies without further preparation. Vapour-quenched films were removed from NaCl substrates by dissolving the substrates in distilled water. These samples were separately annealed in vacuum (about 10^{-2} Torr) at appropriate temperatures and examined in an electron microscope.

For differential thermal analysis (DTA) a Stanton Redcroft DTA 673-4 instrument was used. Liquid-quenched specimens were prepared by breaking the as-quenched foils into small pieces and vapour-quenched specimens were obtained in powder form on removing from the glass slide substrates. Specimens were transferred to the quartz crucibles of the DTA apparatus and an equal weight of pure alumina powder was used as the reference sample. A uniform heating rate of 10° C min^{-1} was used in all cases and all DTA measurements were made in vacuum (about 10^{-2} Torr). The heat of transformation was obtained by calibrating the instrument for melting endotherms of pure Pb and Sn standards.

3. Results and discussion

3.1. Liquid-quenched foils

3.1.1. As-quenched specimens

Continuous scanning diffractometer traces of liquid-quenched foils containing upto about 12.5 at% Ge showed only diffraction maxima corresponding to an fcc structure. In these specimens no peaks were identified which could be interpreted as arising from Ge or any other phase. However, the foils containing $\geqslant 15$ at% Ge gave reflections of Ge also, the intensity of these reflections increasing with increasing Ge concentration. Step scanning over the range of 2θ in which each peak occurred enabled the position of the peaks to be determined accurately. The peak position was taken as being the mid point of the width of the peaks at half maximum intensity above the background. The lattice parameter was determined from each peak and an average value was calculated. Fig. 1 shows the variation of lattice parameter versus Ge concentration for the Pb-rich fcc phase. Lattice parameter decreases up to about 13 at% Ge indicating that about 13 at% Ge can be retained in the Pb-rich fcc phase by liquid-quenching.

In Ge-rich compositions, the diffractometer traces of liquid-quenched foils containing 2.5 at% Pb showed diffraction maxima corresponding to both fcc Pb and cubic Ge. The lattice parameter of the cubic Ge phase in these foils was the same as that of pure quenched Ge.

TEM studies of liquid-quenched foils were made only in thin regions ($\leqslant 0.1$ μm). Specimens of pure Pb revealed the presence of both equilibrium fcc and metastable hcp phases (which is known to stabilize only in electron transparent regions [3]). With increasing Ge concentration the proportion of hcp phase decreases and no evidence of hcp phase was found in alloys containing $\geqslant 7.5$ at% Ge. This observation suggests that addition of Ge in Pb suppresses the stabilization of the hcp phase.

Reflections due to Ge were not observed in foils containing upto about 15 at% Ge. The electron micrographs showed a fine-grained (100–500 Å) well defined single phase within which no second phase precipitation was observed. A typi-

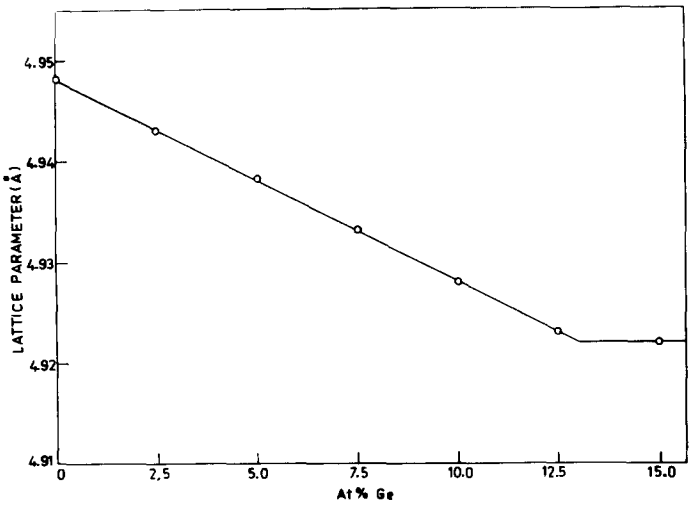

Figure 1 Lattice parameter versus Ge concentration for liquid-quenched Pb-rich fcc phase.

cal electron micrograph and corresponding electron diffraction pattern for as-quenched Pb–15 at% Ge alloy is shown in Fig. 2. These observations indicate a higher value of solid solubility in electron transparent regions. This may presumably be due to higher quenching rates in these regions.

Splat-quenched pure Ge produced only the stable crystalline phase and no evidence was found for the amorphous phase reported by Davies and Hull [8]. In Ge–2.5 at% Pb alloy, both f c c Pb and cubic Ge phases were observed. Segregation of Pb in electron transparent regions also shows that crystalline Ge can not retain even a small amount of Pb, however, as shown later, the crystallized Ge phase (obtained on heating amorphous films) can retain up to about 7.5 at% Pb.

3.1.2. Isochronal annealing

In order to determine the temperature of precipitation of the Pb-rich fcc solid solution, as-quenched alloys were heated isochronally. Absolute value of resistivity and its change on isochronal annealing could not be determined due to varying thickness and porosity of the as-quenched foils. However, a qualitative variation of resistance with temperature was obtained by averaging the measurements of a large number of foils. Fig. 3 shows typical behaviour of a liquid-quenched Pb–10 at% Ge alloy at a heating rate of about 10° C min^{-1}. Only one broad annealing stage is obtained between 220 and 300° C. DTA thermograms of as-quenched foils also indicated a small exothermic hump at about 220° C.

3.1.3. Isothermal annealing

Insothermal decomposition of the Pb–Ge solid solutions was studied by annealing the as-quenched foils at 200, 250, 300 and 350° C for 30 min in each case. Fig. 4 shows the change in X-ray diffraction patterns of Pb–10 at% Ge alloy foils on an-

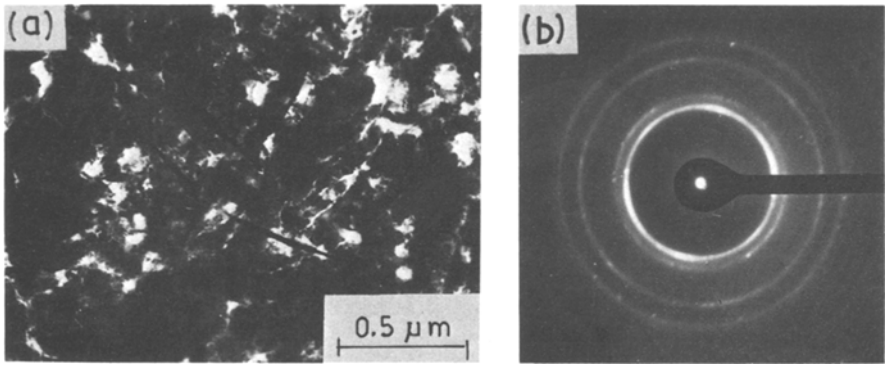

Figure 2 (a) Typical electron micrograph and (b) corresponding electron diffraction pattern of as-quenched Pb–15 at% Ge showing a uniform single fcc phase in electron transparent regions.

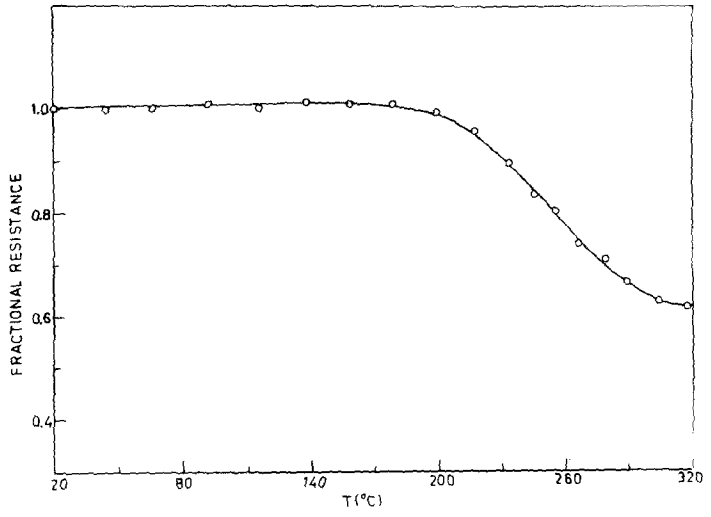

Figure 3 Typical effect of isochronal annealing (10° C min^{-1}) on resistivity of liquid-quenched Pb–10 at% Ge.

nealing at different temperatures. Samples annealed at 200° C (curve 1) show diffraction maxima corresponding to an *fcc* phase only and no Ge reflections are observed. However, in samples annealed at higher temperatures (curves 2 to 4), reflections due to Ge start appearing, the intensities of these reflections increase with increasing annealing temperature. Microstructural

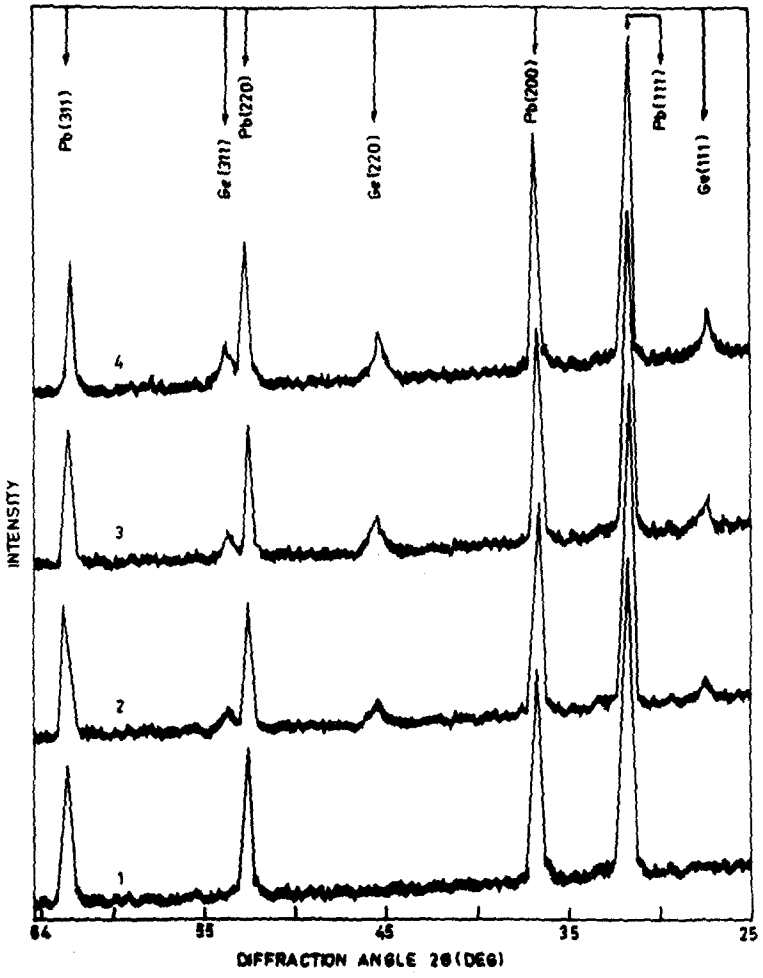

Figure 4 X-ray diffractometer traces of liquid-quenched Pb–10 at% Ge annealed for 30 min at (1) 200, (2) 250, (3) 300 and (4) 350° C.

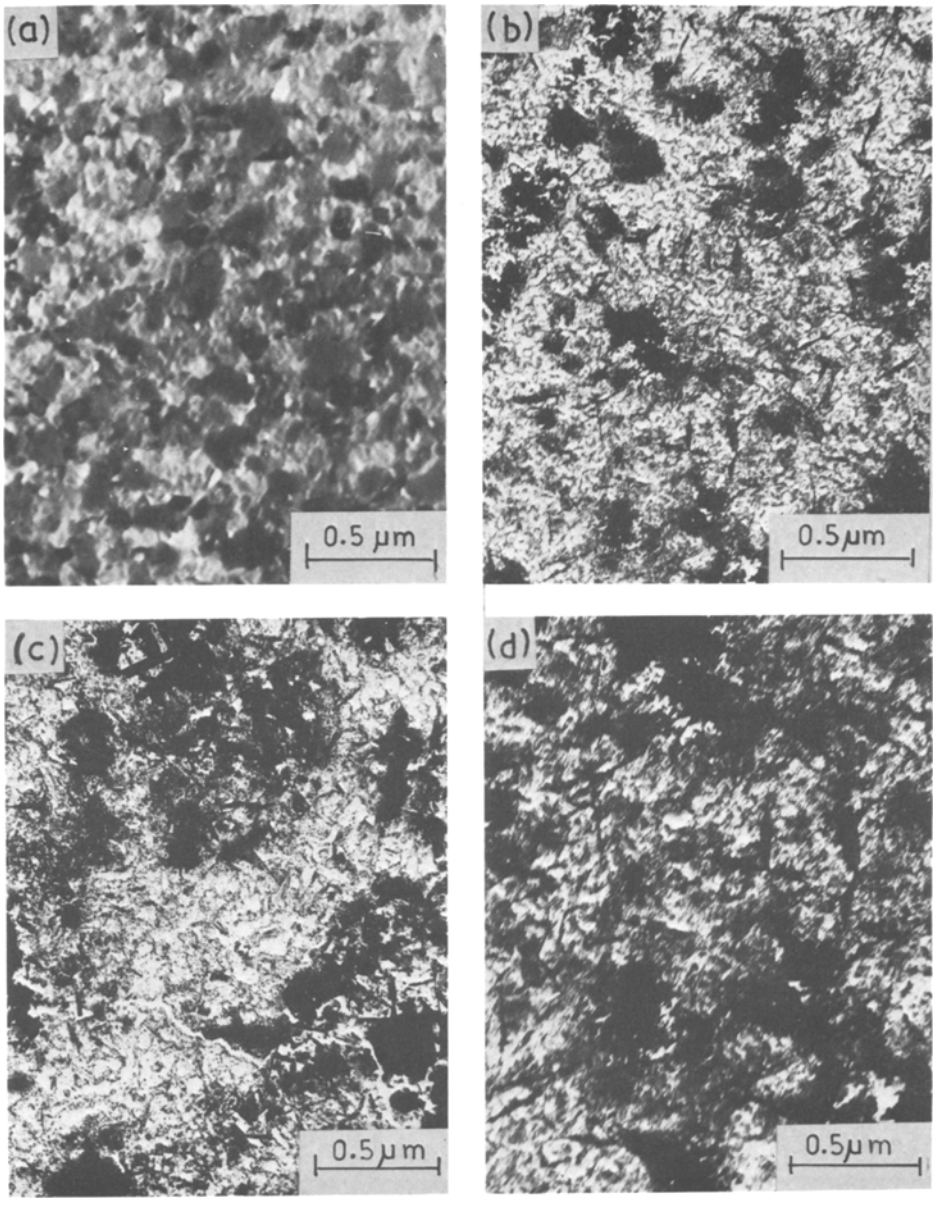

Figure 5 Electron micrographs of liquid-quenched Pb–10 at% Ge annealed for 30 min at (a) 200, (b) 250, (c) 300 and (d) 350° C.

features of Pb–10 at% Ge alloy foils on annealing are shown in Fig. 5. The grain size of as-quenched foils of different compositions was of the same order (100–500 Å) and a typical micrograph of as-quenched Pb–15 at% Ge has already been shown in Fig. 2a. The grain size increases (to 1000–2000 Å) on annealing at 200° C and no phase separation is observed (Fig. 5a). Upon annealing at higher temperatures, the supersaturated fcc phase decomposes and Ge precipitates out (Figs. 5b to d). The size of precipated Ge clusters increases with increasing anneal temperature. The above observations suggest that the precipitation of the Pb-rich solid solution starts above 200° C and is a temperature dependent nucleation and growth phenomenon. An accurate measurement of lattice parameters of annealed samples followed by detailed microscructural studies may throw light on the segregation phenomenon. Such work is in progress.

TABLE I Diffraction peak positions for amorphous Ge-Pb alloy films, K_1: 1st peak, K_2: 2nd peak, $K = 4\pi \sin\theta/\lambda$ (Å^{-1})

Composition	K_1	K_2	K_2/K_1
Ge	1.88	3.45	1.83
Ge–2.5 wt% Pb	1.93	3.52	1.82
Ge–5 wt% Pb	1.97	3.55	1.80
Ge–7.5 wt% Pb	2.02	3.61	1.78

3.2. Vapour-quenched films

3.2.1. As-quenched specimens

Vapour-quenched films were examined only by TEM. For Pb-rich compositions, electron diffraction and microscopy revealed the presence of a single fcc phase upto about 5 at% Ge. Alloy films containing $\geqslant$ 7.5 at% Ge revealed the presence of segregated Ge particles which suggests that by vapour-quenching only about 5 at% Ge can be retained in the Pb-rich fcc solid solution. The variation of lattice parameter versus Ge concentration of the metastable fcc solid solution was found to be approximately the same as for liquid-quenched solid solutions.

For Ge-rich compositions, vapour-quenched films were amorphous upto about 7.5 at% Pb. Above this concentration, segregated Pb and Ge stable phases were observed. Vapour-quenched Ge and alloy films with composition 2.5, 5 and 7.5 at% Pb were studied in detail. These films showed no specific microstructural features at magnifications upto x 200 000. Selected area diffraction from these films consisted of diffuse rings, characteristic of a non-crystalline phase. The positions of the first two peaks were determined from microdensitometer traces of the patterns and expressed in terms of diffraction coordinates $K = 4\pi \sin\theta/\lambda$. Values for first and second diffraction peaks K_1 and K_2, respectively and their ratio K_2/K_1 at different Pb concentrations are listed in Table I. It is noteworthy that the values of K_1 and K_2 increase and their ratio K_2/K_1 decreases with increasing Pb concentration.

3.2.2. Isochronal annealing

The decomposition behaviour of vapour-quenched Pb-rich fcc solid solution was the same as observed for the liquid-quenched foils.

Fig. 6 shows DTA thermograms for the transformation of amorphous Ge and alloy films. The peak at 410° C in curve 1 corresponds to the crystallization of amorphous Ge and the first peak in other curves corresponds to the crystallization of alloy films (as discussed later). The crystallization temperature (T_c) and heat of transformation (H_c) decrease with increasing metal concentration. Variation of T_c and H_c with Pb concentration is shown in Fig. 7. The second exothermic peak (except curve 1) is small and broad. The area of this peak increases and its position shifts slightly towards lower temperatures with increasing Pb concentration. As shown later, this peak corresponds to the precipitation of Pb from supersaturated crystallized Ge.

3.2.3. Isothermal annealing

With the aim of recording the structural changes associated with exothermic DTA peaks, as-quenched films were isothermally annealed in vacuum (about 10^{-2} Torr) for 15 min at tempera-

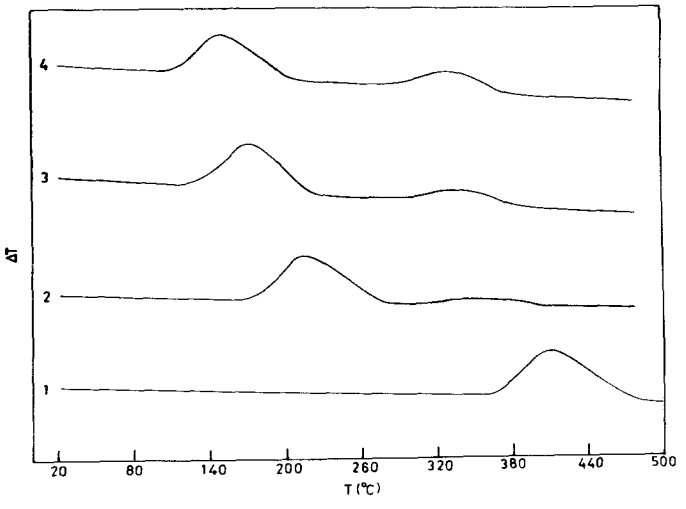

Figure 6 DTA thermograms for vapour-quenched amorphous (1) Ge, (2) Ge–2.5 at% Pb, (3) Ge–5 at% Pb and (4) Ge–7.5 at% Pb films.

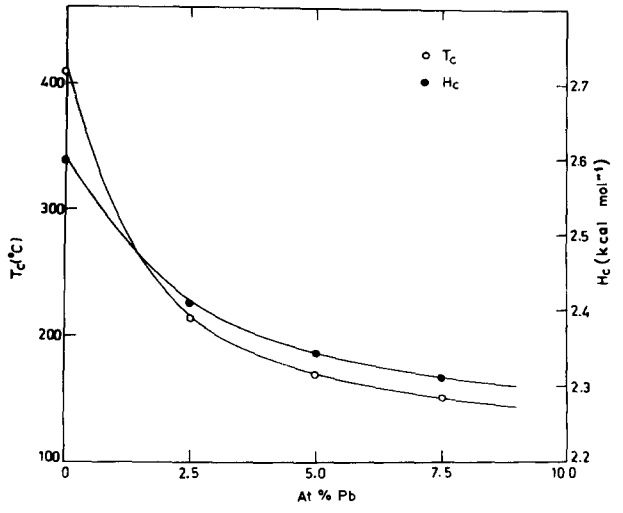

Figure 7 Concentration dependence of T_c and H_c in vapour-quenched amorphous Ge–Pb alloy films.

tures corresponding to peak positions in the differential thermogram. The peak at 410° C in curve 1 was found to be due to crystallization of amorphous Ge. Fig. 8 shows typical electron micrographs and corresponding electron diffraction patterns of as-quenched (a, b) and annealed (c to f) Ge–5 at% Pb alloy films. It is clear from the figure that the film heated to 220° C (above the first DTA peak) gives a diffraction pattern (Fig. 8d) corresponding to that of crystalline Ge. The rings are broad due to the small grain size and the corresponding electron micrograph (Fig. 8c) shows a well defined single phase within which no second phase precipitation is observed. Diffraction patterns of films heated to 370° C (above the second DTA peak) contain rings corresponding to Ge and a (2 0 0) reflection of Pb (Fig. 8f). Upon heating at this temperature, the supersaturated cubic Ge phase starts to decompose and Pb precipitates out as can be clearly seen (Fig. 8e).

3.3. Discussion

3.3.1. Pb-rich phase

It is quite logical to expect that by rapid quenching from the liquid state, liquidus–solidus transition might be crossed fast enough to prevent nucleation and growth of a second solid phase, and the solute atoms might be trapped in the parent lattice in excess of equilibrium value. The lattice parameter for Pb-rich solid solution decreases with increasing Ge content. This decrease may be due to relaxation of the host lattice when atoms of smaller atomic diameter (Ge = 2.75 Å, Pb = 3.50 Å) replace the Pb atoms in the parent lattice. Such a decrease has also been observed in liquid-quenched Pb-rich solid solutions containing Sn, Sb, Cd and Mg as solutes [9]. The magnitude of the decrease in lattice parameter may not directly be interpreted since, besides the size factor, several other factors such as relative valency and electronegativity also influence the lattice spacings of the solid solutions.

Since the vapour phase has no miscibility restrictions, the process of atom by atom deposition produces homogeneous solid solutions of systems which have essentially no solubility in the solid state. The extent of metastable solid solubility depends on the ratio of the atomic diameters of the components and their crystal structures. Such metastable solid solutions in vapour-quenched Co–Cu and Fe–Cu systems have been reported by Kneller [10, 11]. The larger metastable solid solubility limit (about 13 at%) in liquid-quenched foils as compared to vapour-quenched films (about 5 at%) may be understood in terms of high atom mobility during condensation from the vapour phase resulting in the nucleation of clusters of segregated atoms.

3.3.2. Ge-rich phase

No evidence was found for the amorphous phase of Ge in liquid-quenched specimens reported by Davies and Hull [8]. These authors, however, reported that cooling the substrate to 77 K was necessary to produce the glassy phase. It is interesting to note that Ge cannot retain Pb in its lattice when quenched into crystalline form whereas it can retain as much as 7.5 at% Pb in an amorphous matrix. Vapour-quenched non-crystalline Ge is known [1, 12] to have a short

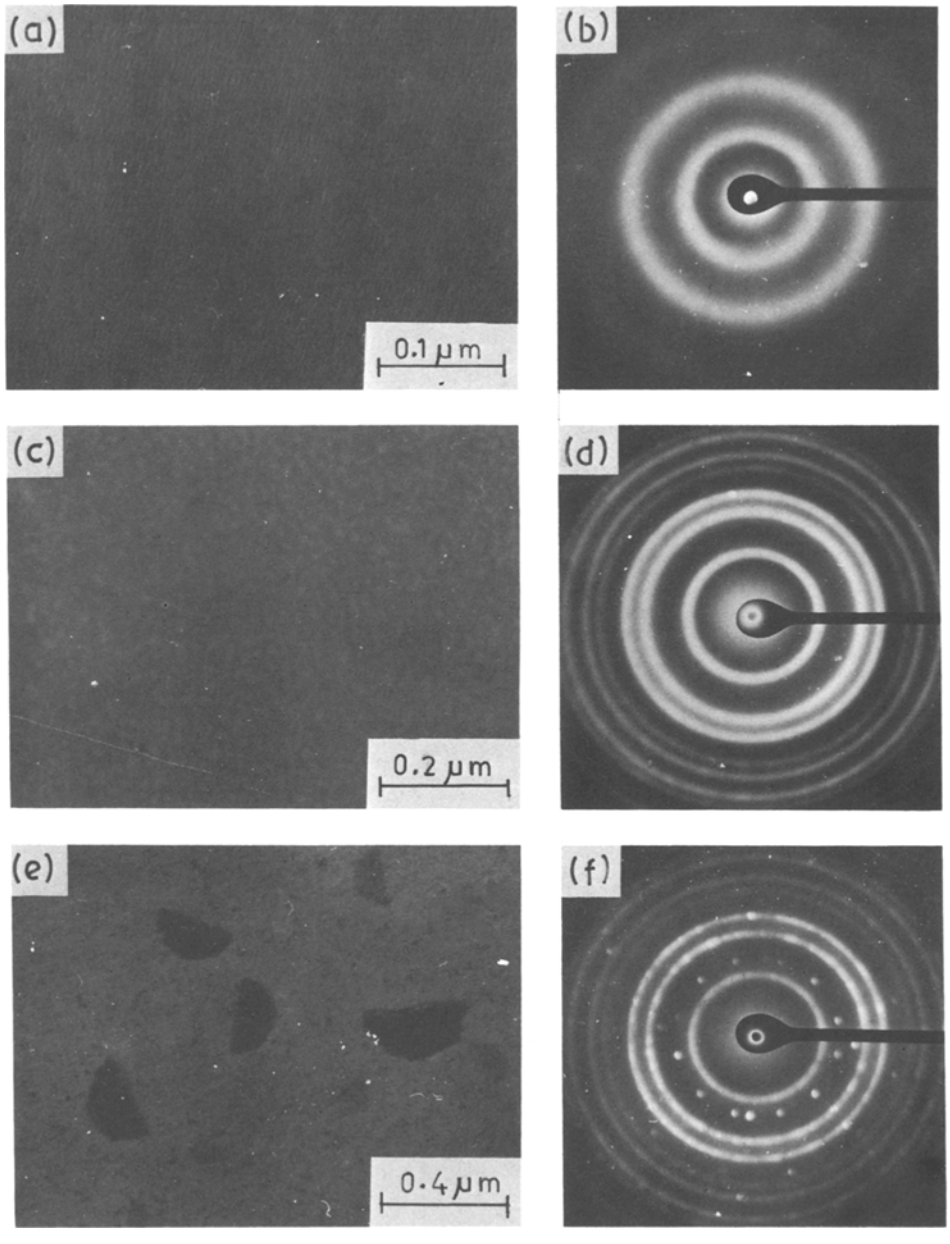

Figure 8 Electron micrographs and corresponding electron diffraction patterns showing amorphous to crystalline transformation in vapour-quenched Ge–5 at% Pb alloy films: (a, b) as-quenched; (c, d) annealed for 15 min at 220° C and (e, f) annealed for 15 min at 370° C.

range, tetrahedral structure similar to that of crystalline Ge. Further, Randhawa *et al.* [13] and Boolchand *et al.* [14] have proposed that the atoms of alloying element are incorporated into an amorphous Ge matrix by replacing the Ge atoms in the tetrahedral sites and/or by going to the voids (empty space between surrounding tetrahedra) and by attaching themselves to the dangling bonds. As there is no metastable solid solubility of Pb in the tetrahedral structure of crystalline Ge, our observation suggests that Pb atoms are incorporated into the amorphous Ge matrix by going into the voids and by attaching themselves to the dangling bonds.

Changes in diffraction coordinates K_1, K_2 and their ratio K_2/K_1 in amorphous Ge–Pb alloy films with increasing Pb concentration may possibly be due to increased packing of atoms and distortion of Ge tetrahedra in the amorphous phase. Results of Koster [15] on amorphous Al–Ge films also

show similar deviations in the first and second diffraction coordinates. Crystallization temperature (T_c) and heat of transformation (H_c) are found to decrease with increasing Pb concentration, similar behaviour has been observed for alloy films of Ge with Fe, Cu, Ag, Au, Ga, In and Nb [13, 16]. The magnitude of decrease in T_c and H_c depends on various parameters like size difference, electronegativity, valency and solubility of the alloying element in crystalline Ge.

Amorphous Ge–5 at% Pb films heated to 220° C (above the first DTA peak) show a single phase crystalline Ge structure, our observations therefore clearly rule out the segregation of alloy films before crystallization. It shows that the crystallized Ge phase can retain upto about 7.5 at% Pb. The question as to whether all the alloying element can be retained in the solid solution on crystallization has been discussed by Koster [15]. A crystal that forms initially in the glassy matrix is termed "polymorphous" if its compostion is still the same as in the glassy matrix and "primary" if the composition has changed. If the composition of the crystals and the amorphous matrix remains the same until 100% of the volume has crystallized i.e. no metal segregation is observed on crystallization, it is termed "polymorphous" crystallization. We may conclude that the transformation of the metastable amorphous Ge–Pb phase into the stable Ge and Pb phases proceeds via polymorphous crystallization of amorphous Ge–Pb into Ge-rich supersaturated solid solution which finally disintegrates into stable Ge and Pb phases. Detailed electrical resistivity and microscopy studies are in progress and may throw light on the kinetics of transformation of amorphous Ge–Pb alloy films.

4. Conclusions

(1) Metastable Pb-rich solid solutions can be produced upto about 13 at% Ge by liquid-quenching and upto about 5 at% Ge by vapour-quenching. Decomposition of the solid solution occurs above 200° C.

(2) Addition of Ge suppresses the stabilization of the metastable hcp phase of Pb.

(3) Amorphous Ge matrix can retain upto about 7.5 at% Pb by incorporating the metal atoms into the voids and/or by attaching to the dangling bonds. Transformation of the amorphous Ge–Pb phase into stable Ge and Pb phases proceeds via polymorphous crystallization of amorphous Ge–Pb into Ge-rich solid solution which finally disintegrates into stable Ge and Pb phases.

Acknowledgements

The assistance of Mr. V. D. Arora, Mr. Mangal Singh and Mr. V. K. Dhar in TEM, DTA and X-ray work is gratefully acknowledged.

References

1. K. L. CHOPRA, "Thin Film Phenomena" (McGraw-Hill, N.Y., 1969).
2. T.R.ANANTHARAMAN and C.SURYANARAYANA *J. Mater. Sci.* **6** (1971) 1111.
3. DILSHAD AKHTAR, V. D. VANKAR, T. C. GOEL and K. L. CHOPRA, *ibid.* **14** (1979) 983.
4. *Idem, ibid.* **14** (1979) 988.
5. *Idem, Thin Solid Films* **58** (1979) 327.
6. M. HANSEN, "Constitution of Binary Alloys" (McGraw-Hill, N.Y., 1958) p. 771.
7. K. L. CHOPRA, P. NATH and A. C. RASTOGI, *Phys. Stat. Sol. (a)* **27** (1975) 645.
8. H. A. DAVIES and J. B. HULL, *J. Mater. Sci.* **9** (1974) 707.
9. N. I. VARICH and A. A. YAKUNIN, *Russian J. Phys. Chem.* **41** (1967) 437.
10. E. KNELLER, *J. Appl. Phys.* **33** (1962) 1355.
11. *Idem, ibid.* **35** (1964) 2210.
12. T. B. LIGHT, *Phys. Rev. Letters* **22** (1969) 999.
13. H. S. RANDHAWA, L. K. MALHOTRA, H. K. SEHGAL and K. L. CHOPRA, *Phys. Stat. Sol. (a)* **37** (1976) 313.
14. P. BOOLCHAND, M. BLIZZARD, H. S. RANDHAWA, D. K. PANDYA, P. NATH and K. L. CHOPRA, Proceedings of the Seventh International Conference on Amorphous and Liquid Semiconductors, Edinburgh (June 1977).
15. U. KOSTER, *Acta Metall.* **20** (1972) 1361.
16. H. S. RANDHAWA, L. K. MALHOTRA and K. L. CHOPRA, *J. Non-Crystal. Solids* **29** (1978) 311.

Received 12 February and accepted 27 March 1980.